AN EXPERIMENTAL STUDY WITH SNUF AND VALIDATION OF THE MARS CODE FOR A DVI LINE BREAK LOCA IN THE APR1400

KEO HYOUNG LEE, BYOUNG UHN BAE, YONG SOO KIM[1], BYONG JO YUN[2], JI HAN CHUN and GOON CHERL PARK*

Department of Nuclear Engineering, Seoul National University,
San 56-1 Sillim-Dong, Kwanak-Gu, Seoul, 151-742, Korea
[1] Korea Hydro & Nuclear Power Co., 25-1, Jang-Dong, Yuseong-Gu, Daejeon, 305-343, Korea
[2] Korea Atomic Energy Research Institute, 1045 Daedeokdaero, Yuseong-Gu, Daejeon, 305-600, Korea
*Corresponding author. E-mail : parkgc@snu.ac.kr

Received September 20, 2007
Accepted for Publication December 22, 2008

In order to analyze thermal hydraulic phenomena during a DVI (Direct Vessel Injection) line break LOCA (Loss-of-Coolant Accident) in the APR1400 (Advanced Power Reactor 1400 MWe), we performed experimental studies with the SNUF (Seoul National University Facility), a reduced-height and reduce-pressure integral test loop with a scaled down APR1400. We performed experiments dealing with eight test cases under varied tests. As a result of the experiment, the primary system pressure, the coolant temperature, and the occurrence time of the downcomer seal clearing were affected significantly by the thermal power in the core and the SI flow rate. The break area played a dominant role in the vent of the steam. For our analytical investigation, we used the MARS code for simulation of the experiments to validate the calculation capability of the code. The results of the analysis showed good and sufficient agreement with the results of the experiment. However, the analysis revealed a weak capability in predicting the bypass flow of the SI water toward the broken DVI line, and it was insufficient to simulate the streamline contraction in the broken side. We, hence, need to improve the MARS code.

KEYWORDS : DVI Line Break LOCA, APR1400, Downcomer Seal Clearing, SNUF, MARS, RHRP Facility, Sensitivity

1. INTRODUCTION

The APR1400 (Advanced Power Reactor 1400 MWe), a next generation nuclear reactor in the Republic of Korea [1], has adopted a DVI (Direct Vessel Injection) system as an advanced feature of its ECCS (Emergency Core Cooling System). In the system, the SI (Safety Injection) water is injected into the reactor vessel downcomer directly from the four DVI nozzles. These nozzles are installed about 2.1 m above the center line of the cold leg instead of using a CLI (Cold Leg Injection) system. Therefore, the DVI system requires an additional safety assessment for a DVI line break LOCA (Loss-of-Coolant Accident).

In a conventional cold leg SBLOCA (Small Break Loss-of-Coolant Accident), the phenomenon of the loop seal clearing in cold legs is crucial. This is because the phenomenon prevents a buildup of steam in the core and enables the coolant level in the core to be maintained enough to recover the fuel [2]. However, in the APR1400 with the DVI system, a downcomer seal exists in the upper downcomer between the cold leg and a broken DVI. Accordingly, the steam generated in the core should pass through the downcomer seal to be released into the containment. The phenomenon of the downcomer seal clearing is that the liquid coolant in the upper downcomer is cleared by the steam flow incoming from the cold legs. The occurrence of this phenomenon can decrease the differential pressure between the core and the downcomer and make the fuel recoverable by the liquid coolant. Therefore, the downcomer seal clearing has an important role on the integrity of fuel during the accident.

Previous studies on this accident focused only on a one-dimensional system code analysis [3, 4] or an air-water separate effect experiment [5]. Thus, an integral effect test and analysis, with the same working fluid, are necessary to validate the performance of the DVI system. Moreover, it is necessary to precisely estimate the sensitivity according to the diverse states of the accident dependent on conditions such as the thermal power, the SI flow rate, the break area, and so on. Hence, this study focused on integral steam-water experiments involving sensitivity analyses with various test conditions to investigate

the phenomena in a DVI line break LOCA.

As a small-scale integral loop test facility, the SNUF (Seoul National University Facility) was utilized for this study [6, 7]. The facility was a kind of RHRP (Reduced-Height and Reduced-Pressure) facility. An energy scaling method, developed in the authors' previous study [8], was adopted to determine the test conditions. According to the test conditions, experimental studies for eight cases were performed with the SNUF. Additionally, some of the experimental results were simulated with the MARS code to validate the calculation capability of the MARS code.

2. EXPERIMENT

2.1 Description of the SNUF

The SNUF test facility is an RHRP integral loop test facility designed to simulate the APR1400 pressurized water reactor. A schematic of the SNUF is shown in Fig. 1. The scaling factors of length and area in the primary system are 1/6.4 and 1/178 with respect to the prototype. The geometrical configuration of the SNUF is equivalent to that of the APR1400, which consists of two hot legs and four cold legs. The test vessel contains 260 heaters to simulate the core decay heat. The maximum total operation power of the heaters is 200 kW, and the maximum operation pressure is 0.8 MPa. The three intact DVI lines can supply the SI water into the upper downcomer, as shown in Fig. 2. The one broken DVI line is connected to the discharge tank. The steam generator, in each loop, contains 16 U-tubes. The major design parameters of the SNUF are listed in Table 1.

In the instrumentation system of the SNUF illustrated in Fig. 3, the differential pressure (DP) transmitters of Rosemount Co. (4EA) were used to measure the collapsed water level in the core and downcomer and the differential pressure between the core and the downcomer. The upper plenum pressure and the discharge tank pressure were

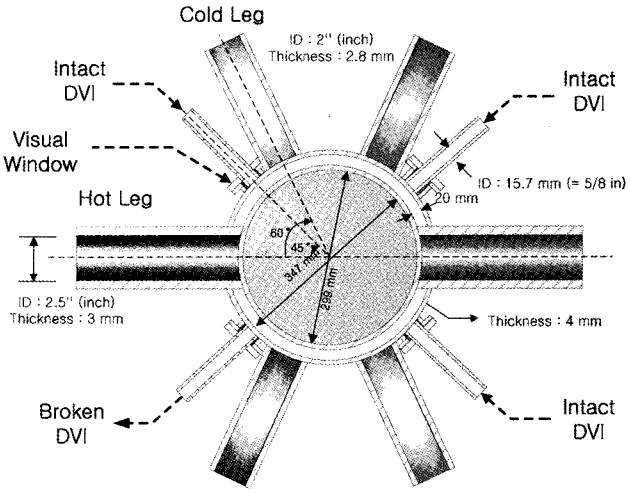

Fig. 2. Plane View of the SNUF

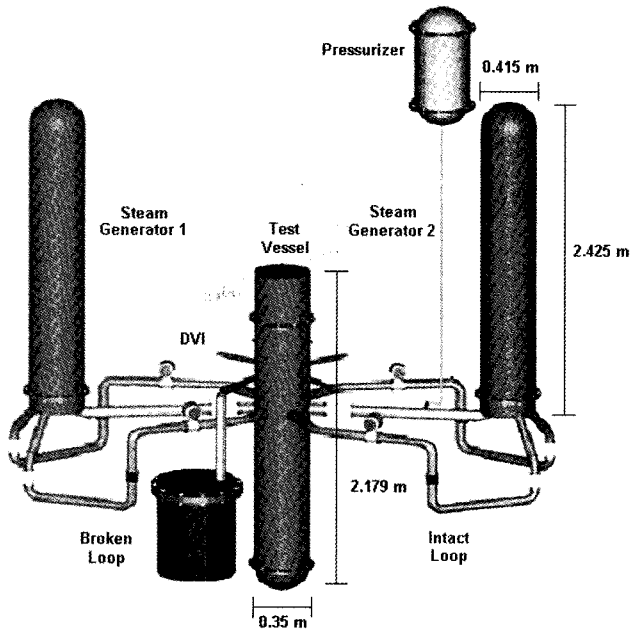

Fig. 1. Schematic Diagram of the SNUF

Table 1. Major Design Characteristics

Parameter	Prototype	SNUF
Number of loops	2	2
Volume scale	1	1/1139.2
Area scale	1	1/178
Height scale	1	1/6.4
Core height [m]	3.81	0.6
Primary side volume [m^3]	368.78	0.226
Core volume	122.24	0.117
Downcomer volume	36.64	0.034
Hot leg volume	11.09	0.007
Cold leg volume	28.17	0.017
U-tube volume	155.58	0.049
Downcomer gap size [m]	0.255	0.020
Hot leg diameter [m]	1.067	0.064
Cold leg diameter [m]	0.762	0.051

measured with the pressure transmitters of the VPRNP-A3 model of the VALCOM Co. (3EA). The temperature of the coolant was measured using K-type thermocouples (42 EA) in the upper plenum, downcomer, cold leg, hot leg, steam generator primary exit, and steam generator secondary side. The SI flow rate was measured by a vortex flowmeter from the OVAL Co. (1EA). The detailed descriptions of the SNUF are explained in Kim et al.'s research [6].

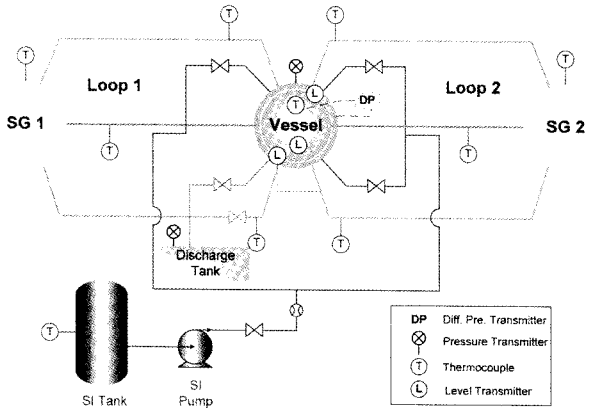

Fig. 3. Instrumentation System of the SNUF

2.2 The Test Conditions of SNUF

To determine the test conditions according to the energy scaling method, it was necessary to obtain the transient results of the thermal-hydraulic phenomena in a prototype for simulating those phenomena in a small scale facility. MARS [9], a thermal hydraulic system analysis code, was utilized in this study for analyzing the DVI line break LOCA in the APR1400 reactor. The code was

Table 2. Initial Conditions of the Prototype Analysis

Parameters	Values
Initial primary system pressure [bar]	157.4
Initial secondary system Pressure [bar]	69.0
Initial core power [MW_{th}]	4062.66
Initial hot leg temperature [°C]	324.53
Initial cold-leg temperature [°C]	290.85
Total HPSI flow rate [kg/s]	57.40
Total SIT flow rate [kg/s]	105.46
SI temperature [°C]	48.9
Initial broken DVI area [m^2]	0.036591

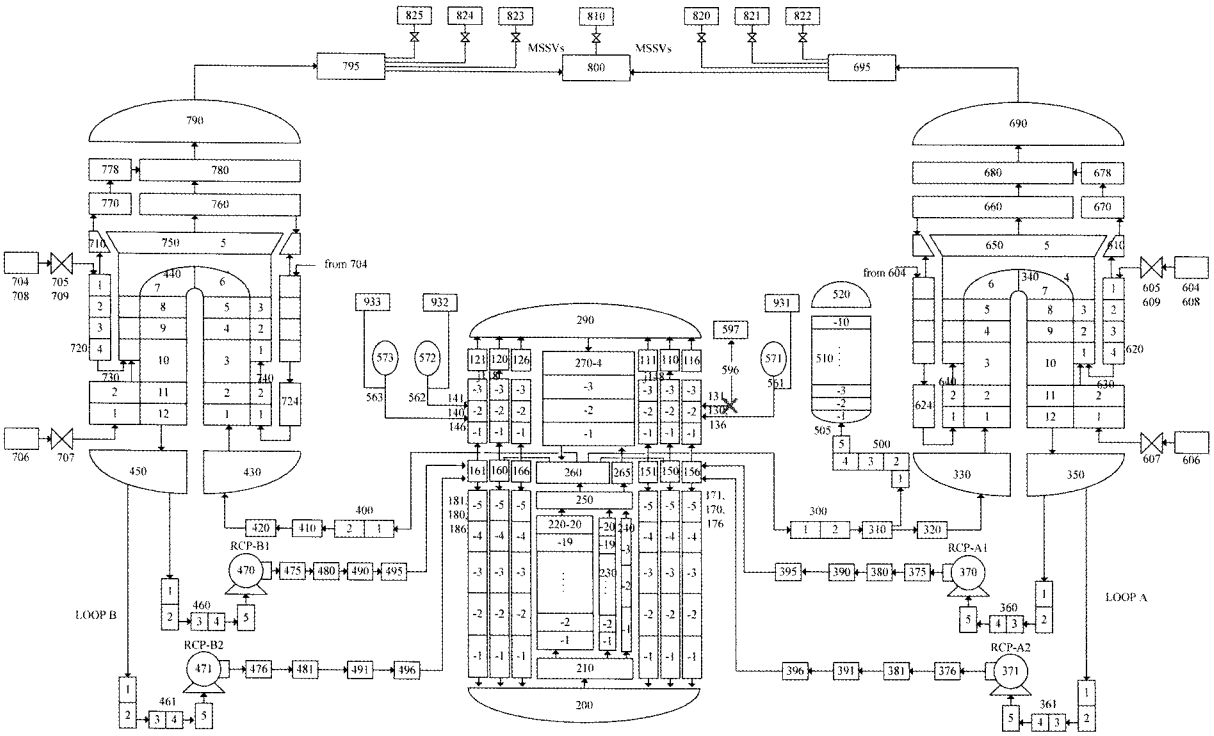

Fig. 4. Nodalization for the APR1400

Table 3. Sequence of Trips in the APR1400

Parameters	Time	Note
Reactor trip	20.968 s	Low pressurizer pressure (P_{PZR}<10.72MPa)
Turbine trip	21.113 s	0.145 s after the reactor trip
RCP trip	21.470 s	0.50 s after the reactor trip
HPSI injection	60.968 s	40.0 after the reactor tip
SIT valve open	240.790 s	Low pressure of SIT inlet (P_{SI}<4.03MPa)

Table 4. Test Conditions of the Base Case

Parameters	Values	Descriptions
Test time [s]	Starting at 30 s after break	To apply lower thermal power
Initial primary system pressure [MPa]	0.6	1/13 (Pressure ratio)
Initial coolant temperature [°C]	158	
Initial secondary temperature [°C]	158	
Thermal power [kW]	110 (0 ~ 60 s) 70 (60 ~ 300 s) 60 (300 ~ 500 s)	Applying an integrated value (3 steps)
HPSI flow rate [kg/s]	0.13	Applying an integrated value
SIT flow rate [kg/s]	0.11	
SI temperature [°C]	27.4	
Broken DVI area [m^2]	0.000177	Henry-Fauske critical flow model
Discharge coefficient	0.62	Considering the streamline contraction
L/D of broken DVI	5.9	

developed at KAERI (Korea Atomic Energy Research Institute), adopting RELAP5 [10] and COBRA-TF [11] as a one-dimensional module and a three-dimensional module, respectively. The geometric nodalization of MARS for the APR1400 system was prepared by KAERI, as shown in Fig. 4. For conservative conditions, we assumed that the core power was 102% of the normal power and 120% of the decay heat according to the ANS73 model [12]. A Guillotine-break of the DVI line was postulated for the most severe case of the DVI line break LOCA. From results of the previous study [8], the initial conditions of the analysis are listed in Table 2 and the sequence and condition of trips in the prototype analysis are summarized in Table 3.

For simulating the accident scenario reasonably in the facility, an appropriate scaling method should be applied. Considering that the SNUF is a kind of RHRP facility, an energy scaling method was proposed to determine the test conditions [8]. This scaling method conserved the total energy as well as the mass inventory of the coolant in the primary system with a prototype. Therefore, the differences of the coolant properties such as the specific volume and the specific enthalpy between the reduced-pressure test facility and the prototype were conserved with the scaling method. This scaling method was derived by taking a non-dimensional formulation of the coolant mass and energy in the system. The scaling factors with respect to the safety injection flow, the size of the broken DVI line, and thermal power in the core were determined to satisfy following relations:

$$\left(\frac{\tau \dot{m}_{in}}{M_0}\right)_R = 1, \quad \left(\frac{\tau \dot{m}_{out}}{M_0}\right)_R = 1, \quad \left(\frac{\tau Q}{M_0 h_c}\right)_R = 1 \qquad (1)$$

Table 5. Variation of the Test Condition According to the each Sensitivity Case

Case number	Case name	Varied Parameters *	Values	Comparison with the base case
P1	The case of the integrated power	Power	70 kW (0 ~ 500 s)	Integrated
P2	The case of reduced power	Power	80 kW (0 ~ 60 s) 40 kW (60 ~ 300 s) 30 kW (300 ~ 500 s)	30 kW lower
B1	The case of reduced break area	Broken DVI area	0.000078 m^2	44%
B2	The case of extended break position	L/D of DVI line	17.7	300%
S1	The case of reduced SI flow rate	HPSI flow rate	0.07 kg/s	54%
		SIT flow rate	0.08 kg/s	73%
S2	The case of increased SI flow rate	SIT flow rate	0.32 kg/s	246%
		SIT flow rate	0.18 kg/s	164%
S3	The case of high temperature of the SI water	SI Temperature	54.6℃	199%

* With respect to the base case in Table 4.

In the above equations, the subscript R is the ratio between the test facility and the prototype. The term, τ, is a time scale. For a real time simulation, the test facility and the prototype should use the same time scale, that is, $\tau_R = 1$. M_0 is the initial coolant inventory in the primary system. The equations are composed of the inlet mass flow ($\dot{m}_{in}$) and the outlet mass flow ($\dot{m}_{out}$) to the system. In a DVI line break accident, the safety injection from three intact DVI lines is the inlet flow, and the discharge flow through the broken DVI is the outlet flow. When the inlet and outlet mass flows in the facility are scaled with Eq. (1), the total coolant inventory ratio between the test facility and the prototype can be conserved during an accident. From the viewpoint of thermal power (Q), the energy balance in the primary system was formulated with respect to a specific enthalpy of the coolant (h_c) and the total mass of coolant in the system. According to the energy scaling method, the detailed test conditions were determined from scaling down the thermal-hydraulic conditions of the prototype analysis [13], as summarized in Table 4. The thermal power and the SI flow rate among the parameters were determined as the integrated values. As shown in Figs. 5-6, the core power changed continuously, and the SI flow rate oscillated after 210 s in the prototype. It was not easy to precisely simulate the power curve and the oscillation of the flow rate in the actual facility, so the integrated values were supplied.

This scaling method was developed to conserve the total energy as well as the mass inventory of the coolant in the primary system with a prototype. Therefore, the differences of the properties of water such as the specific volume and the specific enthalpy between the reduced-pressure test facility and the prototype can be conserved with the scaling method.

2.3 The Test Matrix

Prior to the sensitivity tests, the base test case according to the conditions in Table 4 was performed to simulate the DVI line break accident of the prototype analysis. The results of the base case can be utilized to predict the thermal hydraulic phenomena in the prototype.

On the other hand, the test conditions such as the thermal power, the SI flow rate, the SI temperature, and the break area can affect the major thermal hydraulic phenomenon significantly in the accident. Accordingly, by estimating the influence of each parameter, the thermal hydraulic phenomena during the DVI line break accident can be sufficiently understood for reactor safety. Also, this study focused on validating the capability of the MARS code by comparing it with the experimental results. Therefore, the experiments and the analyses were performed for various test conditions. A total of seven test cases for sensitivity analysis beside the base case were selected in this study, as listed in Table 5, where one condition of the base case was varied for the each sensitivity case.

The experiments for two test cases, using varied thermal power from the base case, were carried out. This was because the thermal power in the core can strongly influence the steam generation rate. This rate is related to the differential pressure between the core and the downcomer and the phenomenon of the downcomer seal clearing. Hence, the case of the integrated power (P1) and the case of the reduced power (P2) were selected for analyzing the sensitivity according to the condition of the

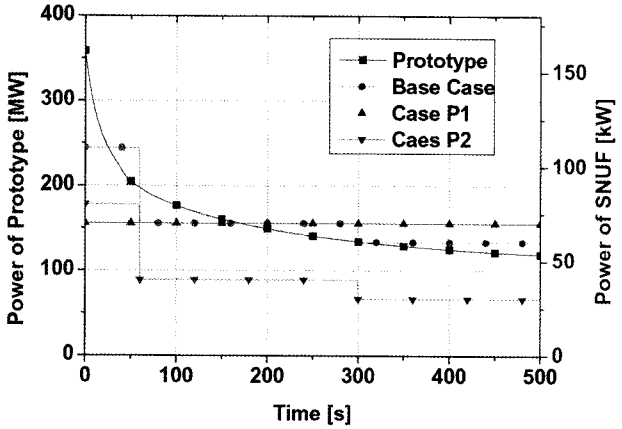

Fig. 5. Supplied Power as Compared to the Case of Variation of Thermal Power

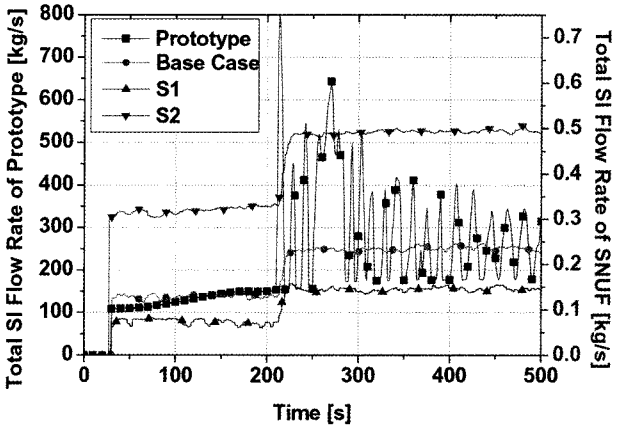

Fig. 6. SI Flow Rate Compared to the Case of Variation of the SI Flow Rate

varied thermal power. In the P1 case, the integrated value of the thermal power, 70 kW, was applied during the entire test period. Thus, in this case, the supplied total energy was the same as that of the base case, but the thermal power before 60 s was low and the thermal power after 300 s was high compared to the base case. In the P2 case, the thermal power, 30 kW lower than the base case, was applied so that the thermal power during the whole period was low compared to that of the base case. The results of the two test cases can be utilized to analyze the influence of various types of supplied power in Fig. 5.

The transient of the coolant inventory during the DVI line break LOCA is governed by the discharge of the coolant for the primary system through the broken DVI line. The discharged flow rate is strongly related to the area of the break. Therefore, we selected the case of the reduced break area (B1) as a sensitivity case. Considering that a Guillotine break of the DVI line was simulated in the base case, the B1 case was to simulate a partial break of the DVI line. In this case, the break area was reduced by the installation of an orifice, and it was 44% of the area of the base case. The position of the break was also an important parameter for the accident. The discharged flow during the accident reaches the critical flow, so that the effect of the L/D (Length / Diameter) ratio of a broken pipe can influence the discharged flow rate [14]. Therefore, the case of the extended break position (B2) was performed with a different broken pipe which has a three times longer length than that of the base case.

In the prototype, the SI water was injected in two ways, HPSI (High Pressure Safety Injection) and SIT (Safety Injection Tank), as listed in Table 3. The HPSI pump operated for about 60 s after the reactor trip. The SIT valves were opened passively at about 240 s when the primary system pressure decreased to less than 4.0 MPa in the prototype. The SI water by the two injection types was injected to the downcomer directly via the DVI line. Because the DVI nozzles were installed above the cold leg, a countercurrent flow occurred in the upper downcomer by the steam flow incoming from the cold leg and the SI flow injecting from the DVI line during the DVI line break LOCA. The downcomer seal clearing occurred when the steam flow penetrated the coolant in the upper downcomer so that the SI flow rate, which is affected the amount of the coolant in the upper downcomer, was one of the governing factors for the downcomer seal clearing. Also, it affected the total energy of the coolant in the primary system. Thus, we performed sensitivity tests on the SI flow rate. To simulate the single failure state when the HPSI water was injected through only one DVI line due to the loss of off-site power, the sensitivity study of the reduced SI flow rate (S1) was carried out. Also, the case of the increased SI flow rate (S2) was investigated to estimate the effect according to the increased SI flow rate. In case S1, 54% of the HPSI flow rate of the base case and 73% of the SIT flow rate of the base case were applied. In case S2, the HPSI flow rate was about 2.5 times larger than that of the base case. The SIT flow rate was about 1.6 times larger than that of the base case. The measured SI flow rates of the two sensitivity cases and the base case are compared in Fig. 6. From the comparison between the base case and the two sensitivity cases, the influence according to the SI flow rate can be analyzed, especially, from the viewpoint of the downcomer seal clearing.

Last, the temperature of SI water was determined by the energy scaling method for conserving the energy of the coolant in the primary system in the base case. According to the method, the temperature of SI water should be 27.4°C. However, in the other study [15], the temperature of the SI water was determined by the subcooling ratio for conserving the amount of the condensation in the upper downcomer:

$$\left(\frac{C_p \Delta T}{h_{fg}} \left(\frac{\rho_f}{\rho_g} \right)^{1/2} \right)_R = 1 \quad \text{, where} \quad \Delta T_R = \frac{\rho_{gR}^{1/2} h_{fgR}}{\rho_{fR}^{1/2} C_{pR}}. \tag{2}$$

According to Eq. (2), the temperature of SI water should be 54.6°C, which is higher than that of the base case. Therefore, the case of the high temperature of the SI water (S3) was performed with the temperature as given in Eq. (2).

2.4 The Experimental Results

2.4.1 The Base Case

To simulate the DVI line break accident as the prototype analysis mentioned in Section 2.2, the base case was performed with the SNUF. The results of the base case can be utilized to experiment with the phenomena in the actual DVI line break accident in the prototype and can be a standard for comparison with the sensitivity test cases.

Figure 7 shows the primary system pressure measured in the upper plenum. The pressure was increased rapidly before 15 s. This increase was due to the experimental procedure at the initiation of the test. In the real test with the SNUF, the thermal power was turned off for setting the exact initial test conditions before starting the test. When the temperatures of all components of the reactor, including the secondary system, became equivalent, the test started and the thermal power was applied. At that time, the flow rate of the loop of the test facility was almost zero without natural circulation. Thus, the thermal power of the core could not be effectively removed to the coolant during the initial period so that subcooled boiling suddenly occurred, and the primary system pressure increased. A procedure for the initiation of the test was attempted to simulate the prototype in the middle of the transient with the test facility. However, the downcomer seal clearing that we focused on in this study occurred after about 70 s. Then, the pressure increase before 15 s did not significantly affect the major thermal hydraulic phenomena in the accident.

The primary system pressure started to decrease after 15 s since the coolant of the primary system was continually discharged into the broken DVI line. Figure 8 shows the coolant temperature of the hot leg. The trend of the coolant

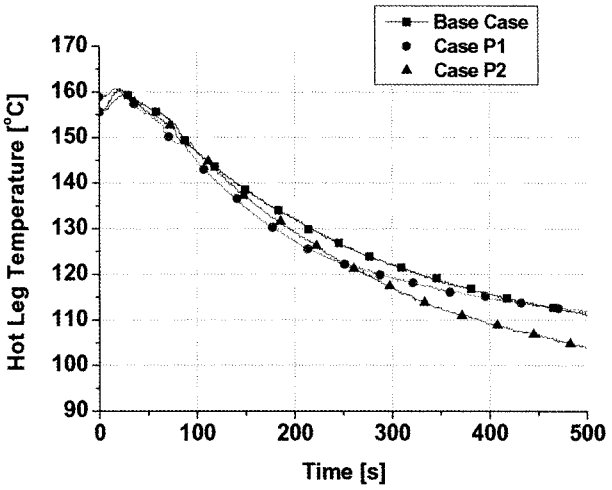

Fig. 8. Hot Leg Temperature Compared to the Case of Variation of Thermal Power

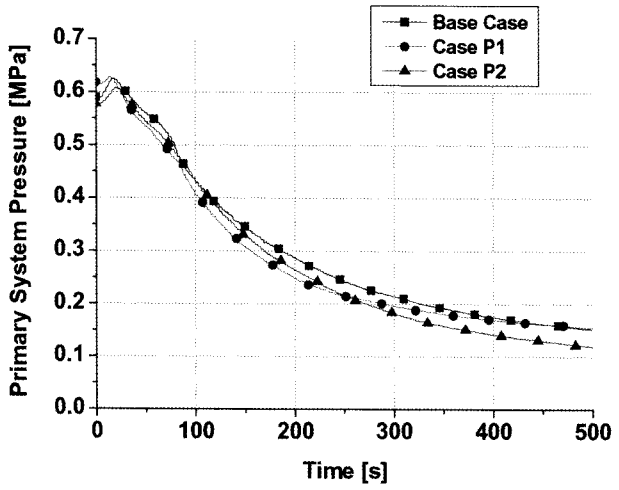

Fig. 7. Primary System Pressure Compared to the Case of Variation of Thermal Power

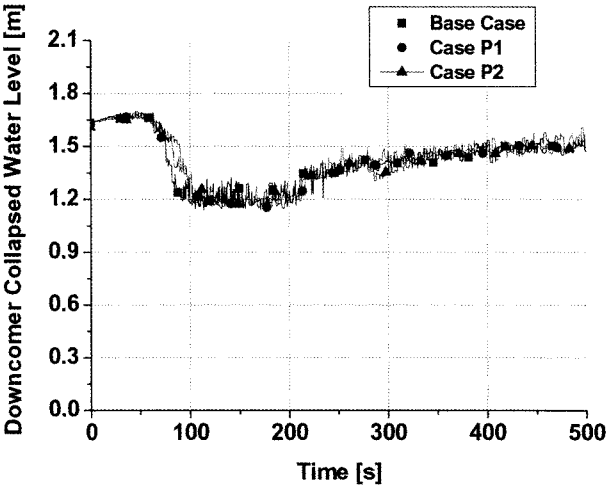

Fig. 9. Downcomer Collapsed Water Level Compared to the Case of Variation of Thermal Power

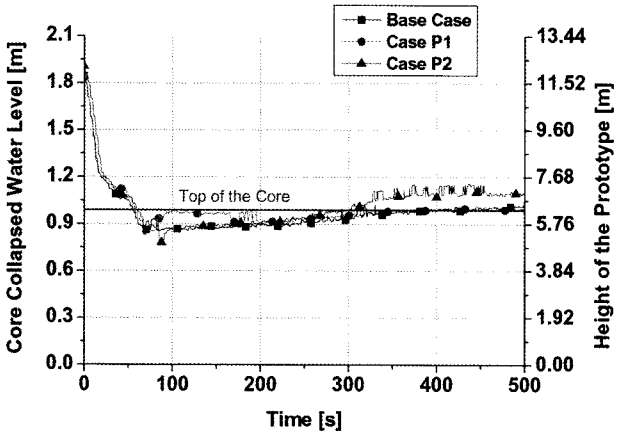

Fig. 10. Core Collapsed Water Level Compared to the Case of Variation of Thermal Power

temperature was similar to the primary system pressure because the coolant of the primary system was saturated during the accident. However, the decreasing rates of the primary system pressure and the coolant temperature before and after 70 s were different. After that time, the downcomer collapsed water level decreased rapidly, as shown in Fig. 9. This rapid decrease meant that the liquid coolant in the upper downcomer was cleared by steam flow incoming from the cold legs; then, the upper downcomer was filled with steam. That phenomenon was the downcomer seal clearing. After the occurrence of this phenomenon, the steam generated in the core could be effectively discharged to the broken DVI line through the loops of the primary system and the upper downcomer. Thus, the system pressure of the core could be decreased rapidly after 70 s, as shown in Fig. 7.

The core collapsed water level decreased rapidly before 70 s, as illustrated in Fig. 10. However, the downcomer collapsed water level did not decrease before 70 s, even though the coolant in the downcomer discharged rapidly. This rapid discharge was due to the differential pressure between the core and the downcomer. The steam generated in the core by the thermal power increased the differential pressure between the core and the downcomer. As a result, the core collapsed water level decreased, and the downcomer collapsed water level was maintained during the initial period of the accident. The downcomer seal clearing occurred at around 70 s. At this time, the differential pressure between the core and the downcomer was reduced, meaning that the core collapsed water lever could be recovered after 70 s, as shown in Fig. 10.

The above results of the base case showed similar trends to the results of the prototype analysis in the previous study [13]. Therefore, we concluded that the DVI line break accident in the prototype, APR1400, was simulated well with the SNUF experiment according to the energy scaling method.

2.4.2 Variation of the Thermal Power

For estimating the effect of thermal power in the core, we carried out cases P1 (integrated power) and P2 (reduced Power) with different types of applied power.

As compared in Figs. 7-8, the primary system pressure and the coolant temperature of case P1 were decreased more rapidly before 200 s than that of the base case. However, the decreasing rates of the parameters started to be less than that of the base case after 200 s. The difference between the base case and case P1 was caused by the amount of thermal power in the core. In case P1, the thermal power was applied less before 60 s and more after 300 s. Because the pressure and the temperature were strongly related to the system energy, the base case and case P1 showed dissimilar trends with respect to the primary system pressure and the coolant temperature.

Figure 10 shows that the core collapsed water level of case P1 was highly maintained between 70 s and 200 s compared to the base case. The lower thermal power was applied in case P1 during the first half period, so we expected that the generation rate of the steam in the core was less than that of the base case before 200 s. Because the amount of the steam in the core was less, and the pressure of the core was lower, the differential pressure between the core and the downcomer was lower than that of the base case before 200 s. The time averaged differential pressures between the upper core and the upper downcomer indicated 1098.6 Pa in case P1, whereas, the pressure before 200 s was 1248.6 Pa in the base case, respectively. Hence, the core collapsed water level was maintained at a high level compared to the base case between 70 s and 200 s. The low differential pressure between the core and the downcomer in case P1 meant that the momentum of the steam to push the coolant in the loop and the upper downcomer was lower than in the base case. Thus, the downcomer seal clearing occurred about 10 s late compared to the base case, as shown in Fig. 9.

On the other hand, the primary system pressure and the coolant temperature of case P2 were decreased more rapidly than that of the base case during all of the accident periods, as shown in Figs. 7-8. These rapid decreases were because the total energy of the primary system was smaller than that of the base case by the reduced thermal power. Since the thermal power was low compared to the base case, the overall generation rate of the steam was also less than that of the base case. This meant that the decreasing rate of the core collapsed water level was low, and the downcomer seal clearing occurred about 20 s late in case P2, as illustrated in Figs. 9-10.

After the water of the SITs started to be injected at about 210 s, the effect, as a consequence of the reduced thermal power, noticeably appeared. Due to water injection from the SITs, the total sensible heat of the coolant in the

primary system decreased rapidly after 210 s. Because the thermal power in case P2 was relatively lower than that of the base case, the supplied energy was insufficient to vaporize the coolant in the core as compared to the base case. Therefore, the coolant in the core was not vaporized sufficiently in case P2. The differential pressure between the core and the downcomer showed lower values than that of the base case after 210 s. The average differential pressure was 437.7 Pa in case P2; whereas it was 607.6 Pa in the base case between 200 s and 500 s. Thus, the core collapsed water level after 210 s was maintained at a high level as compared to the base case illustrated in Fig. 10.

According to the above analyses, the pressure and the temperature of the primary system were directly related to the thermal power in the core. The occurrence time of the downcomer seal clearing was delayed when the thermal power was lower than the base case. The core collapsed water level, an important parameter for reactor safety, showed a trend sensitive to the thermal power in the core.

2.4.3 Variation of the Area and L/D of the Broken DVI Line

The coolant inventory in the primary system is strongly governed by the discharged flow rate. Therefore, in the DVI line break accident, we had to estimate the effect of the discharged flow rate dependent on the break area and position. Thus, case B1 (reduced break area) and B2 (extended break position) were selected for a sensitivity study.

The break area of case B1 was smaller than that of the base case, so we expected that the discharged flow rate to the broken DVI line also decreased. Because the total energy of the coolant in the primary system was relevant to the total mass of the coolant, the total energy of the primary system of case B1 also decreased slowly as compared to the base case. Therefore, the primary system pressure and the coolant temperature of case B1 were also decreased slowly as compared to the base case, as shown in Figs. 11-12.

The upper downcomer was filled with steam when the coolant in the upper downcomer was pushed by the steam, which is forced by the pressure of the core. Therefore, the high differential pressure between the core and the downcomer was beneficial for venting steam. In case B1, the average differential pressure between the upper core and the upper downcomer was 770.9 Pa before 200 s. This value was significantly low as compared to that of the

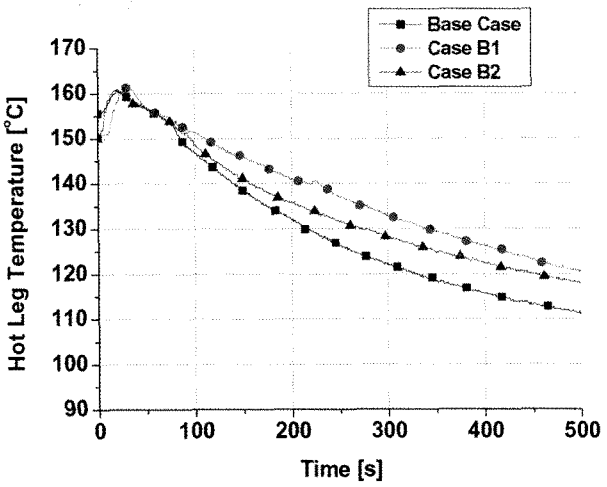

Fig. 12. Hot Leg Temperature Compared to the Case of Variation of the Broken DVI Line

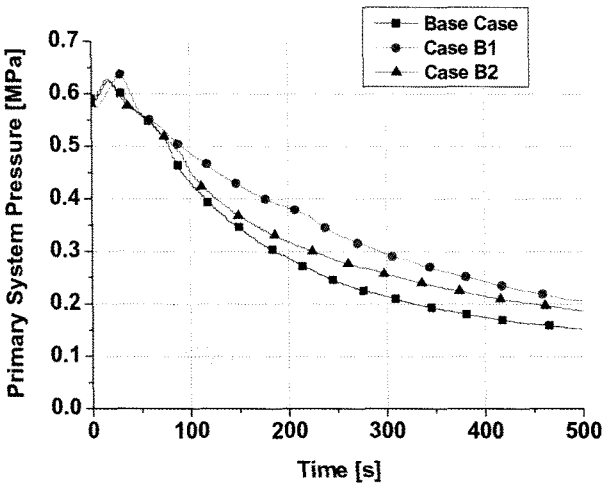

Fig. 11. Primary System Pressure Compared to the Case of Variation of the Broken DVI Line

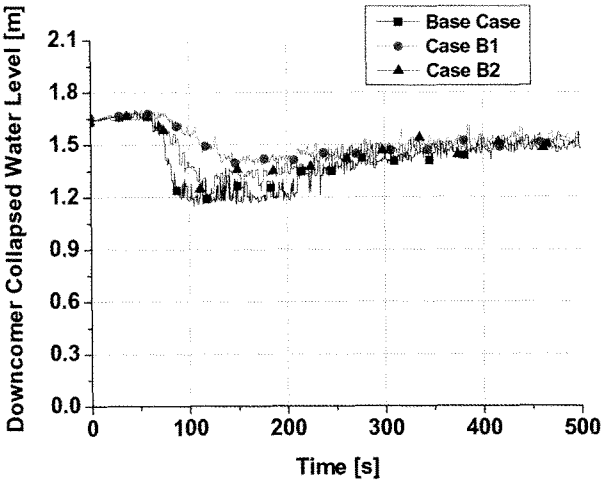

Fig. 13. Downcomer Collapsed Water Level Compared to the Case of Variation of the Broken DVI Line

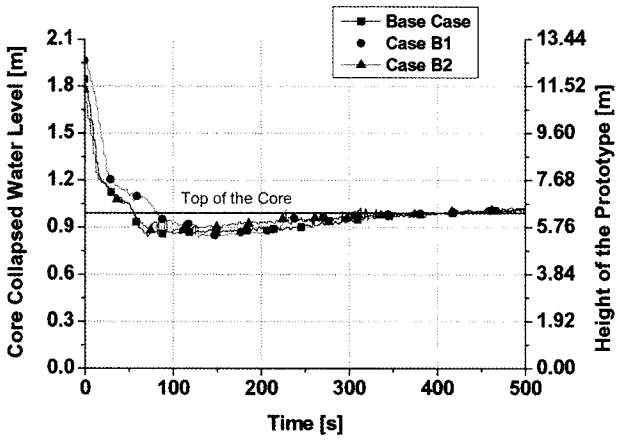

Fig. 14. Core Collapsed Water Level Compared to the Case of Variation of the Broken DVI Line

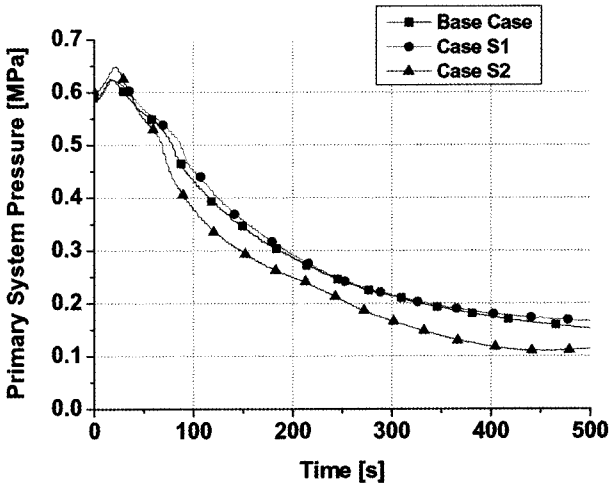

Fig. 15. Primary System Pressure Compared to the Case of the Variation of the SI Flow Rate

base case, 1248.6 Pa. From the results, it can be expected that the amount of the steam in the upper downcomer of case B1 was less than that of the base case. Thus, the downcomer collapsed water level in case B1 maintained a higher level than the base case from 70 s to 250 s, as shown in Fig. 13. Also, the downcomer collapsed water level was not decreased rapidly around 70 s, unlike the base case. In other words, the downcomer collapsed water level decreased slowly from 70 s to 150 s; however, the downcomer collapsed water level decreased rapidly around 70 s in the base case. Thus, the decreasing rate of the primary system pressure did not suddenly change around 70 s as compared and as shown in Fig. 11. On the other hand, the core collapsed water level showed higher values compared to the base case before 100 s, as illustrated in Fig. 14. This was because the total coolant inventory was not decreased as in the base case due to the small break area.

The other factor that affected the discharged flow rate was the L/D ratio of the break line because the mass flux of the critical flow at the broken DVI nozzle is dependent on L/D [14]. The mass flux in a long channel was lower due to the sufficiently long residence time than in a short channel. The L/D ratio was about 6 in the base case and was about 18 in case B2. Therefore, the discharged flow rate to the broken DVI line of case B2 was lower than that of the base case. From the viewpoint of the reduction of the discharged flow rate, cases B1 and B2 encouraged very similar effects in the coolant inventory. The trends of the thermal hydraulic phenomenon also showed similar results, as illustrated in Figs. 11-14. The primary system pressure and the coolant temperature were decreased slowly, and the core and the downcomer collapsed water level were higher than those of the base case.

From the results of the above two sensitivity cases, we concluded that the steam did not vent relatively well

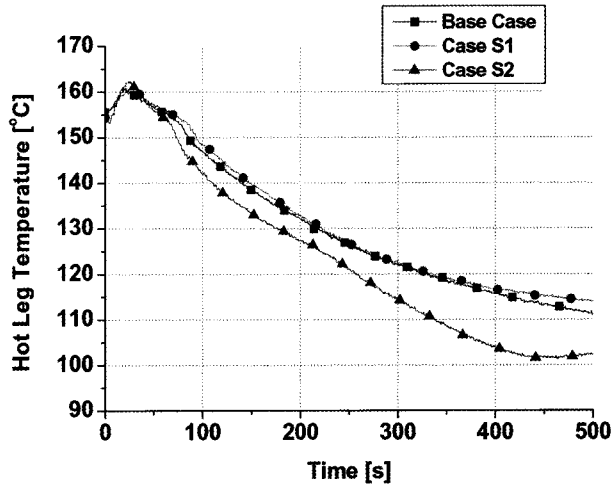

Fig. 16. Hot Leg Temperature Compared to the Case of the Variation of the SI Flow Rate

when reducing the break area or extending the break position when the discharged flow rate through the broken DVI line became low.

2.4.4 Variation of the SI Flow Rate

The DVI system is a new feature for the APR1400. The SI flow rate is an important factor influencing the downcomer seal clearing and the total energy of the primary system. Therefore, the effect as a function of the SI flow rate should be evaluated. In this study, cases S1 (reduced SI flow rate) and S2 (increased SI flow rate) were conducted with different amounts for the SI flow rate.

As illustrated in Figs. 15-16, the primary system pressure and the coolant temperature in case S1 showed almost the same trends as those of the base case. This was true even though a reduced SI flow rate was applied as compared to the base case. This meant that the decrease of the SI flow rate in case S1 did not significantly affect the total energy of the primary system. However, the downcomer seal clearing occurred about 10 s faster, and the downcomer collapsed water level was lower in case S1 than that of the base case, as compared in Fig. 17. This was because the SI flow rate by HPSI, at that time, was low, so that the steam incoming from the cold leg could pass through the water in the upper downcomer more easily in case S1. Figure 18 shows that the core collapsed water level of case S1 was similar to the base case. The minimum core collapsed water level was almost the same between the base case and case S1. This similarity meant that the risk to the reactor core during the single failure state generated by the loss of off-site power was almost equivalent to that during the no failure state.

On the other hand, as shown in Figs. 15-16, the primary system pressure and the coolant temperature of case S2 decreased faster than those of the base case. The total energy of the primary system was decreased more rapidly by the relatively high SI flow rate in case S2. The downcomer seal clearing occurred about 10 s late compared to the base case illustrated in Fig. 17. The steam, incoming from the cold leg, could not pass sufficiently through the upper downcomer due to the significant amount of SI water injected from the intact DVI line. The downcomer collapsed water level of case S2 was higher than that of the base case after 80 s. However, the core collapsed water level was not maintained at a high level compared to the downcomer collapsed water level. Fig. 18 shows that the minimum core collapsed water level was the same as the base case since the steam generated in the core could not be sufficiently discharged by the increased SI water. Therefore, we concluded that the variation of the SI flow rate did not significantly influence the integrity of the fuel during the accident.

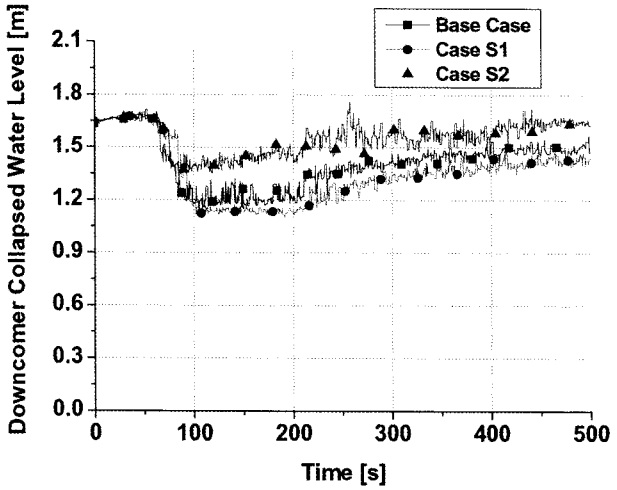

Fig. 17. Downcomer Collapsed Water Level Compared to the Case of the Variation of the SI Flow Rate

2.4.5 Variation of the SI Temperature

The SI water brings about the condensation of the steam incoming from the cold leg so that the temperature

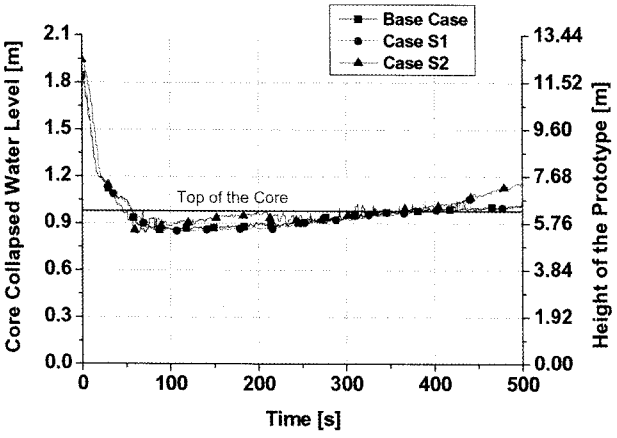

Fig. 18. Core Collapsed Water Level Compared to the Case of the Variation of the SI Flow Rate

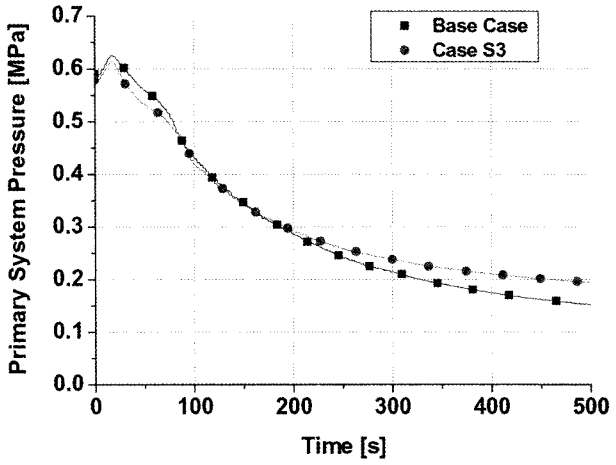

Fig. 19. Primary System Pressure Compared to the Case of the Variation of the SI Temperature

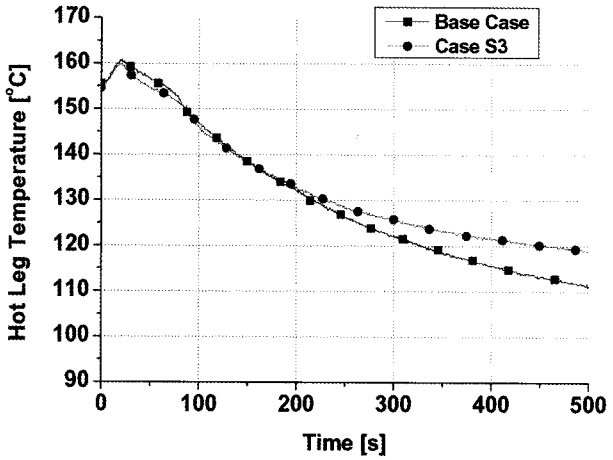

Fig. 20. Hot Leg Temperature Compared to the Case of the Variation of the SI Temperature

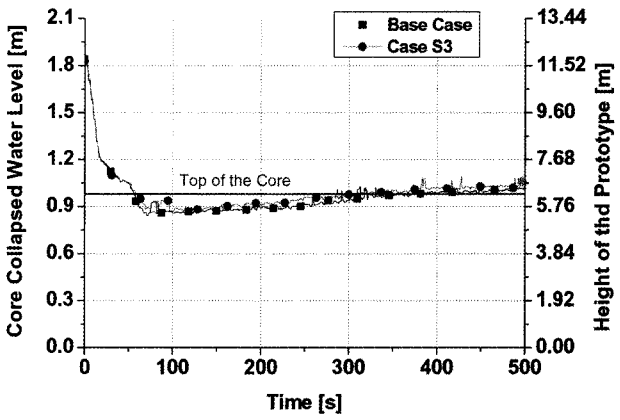

Fig. 22. Core Collapsed Water Level Compared to the Case of the Variation of the SI Temperature

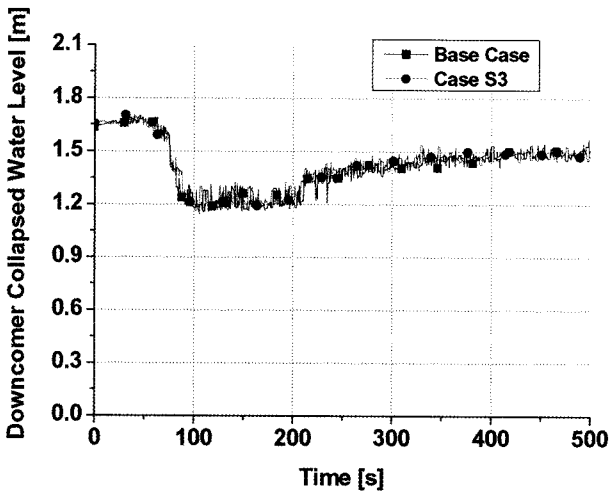

Fig. 21. Downcomer Collapsed Water Level Compared to the Case of the Variation of the SI Temperature

of the SI water can be an important condition in the DVI line break accident. As compared in Figs. 19-22, the results of case S3 (the high temperature of SI water) showed very similar trends to the base case before 200 s. These trends indicated that the temperature of the SI water was not significantly affected by the overall thermal hydraulic phenomena before 200 s. This was because the amount of the injected SI water by the HPSI was not sufficient enough to influence the total energy of the primary system and the downcomer seal clearing. However, the primary system pressure and the coolant temperature decreased slowly after 200 s compared to the base case. This was because the SIT water started to be injected at about 200 s. Water of a higher temperature had a higher specific enthalpy so that the SIT water of case S3 had more energy than that of the base case. This water made the pressure and the temperature decrease slower than in the base case.

According to the above analyses, the temperature of the SI water affected the primary system pressure and coolant temperature in the DVI line break accident after 200 s, but it did not significantly influence the overall phenomena before 200 s. The downcomer seal clearing and the core collapsed water level with respect to the safety of the reactor core were not affected by the temperature of the SI water.

In a previous study [13], the results of the base case experiment showed similar trends to the transient behavior, such as the primary system pressure and the coolant temperature, in the DVI line break LOCA of the prototype. Therefore, the temperature of the SI water which was determined by the energy scaling method was more suitable for observing the overall trends in the reactor. However, when focusing on the local phenomenon in the upper downcomer during the downcomer seal clearing, the condensation of the steam by the SI water is important and the method by using the subcooling ratio should be considered for the separated effect test.

3. VALIDATION OF THE MARS CODE

3.1 SNUF Modeling for Code Assessment

For evaluating the capability of the MARS code, a SNUF experiment was simulated with the MARS program. The nodalization was made, as illustrated in Fig. 23. The SNUF model consisted of a test vessel, two hot legs, two steam generators, and four cold legs. The test vessel consisted of the lower plenum (C160 and C180), core (C190), upper plenum (C210 and C220), upper downcomer

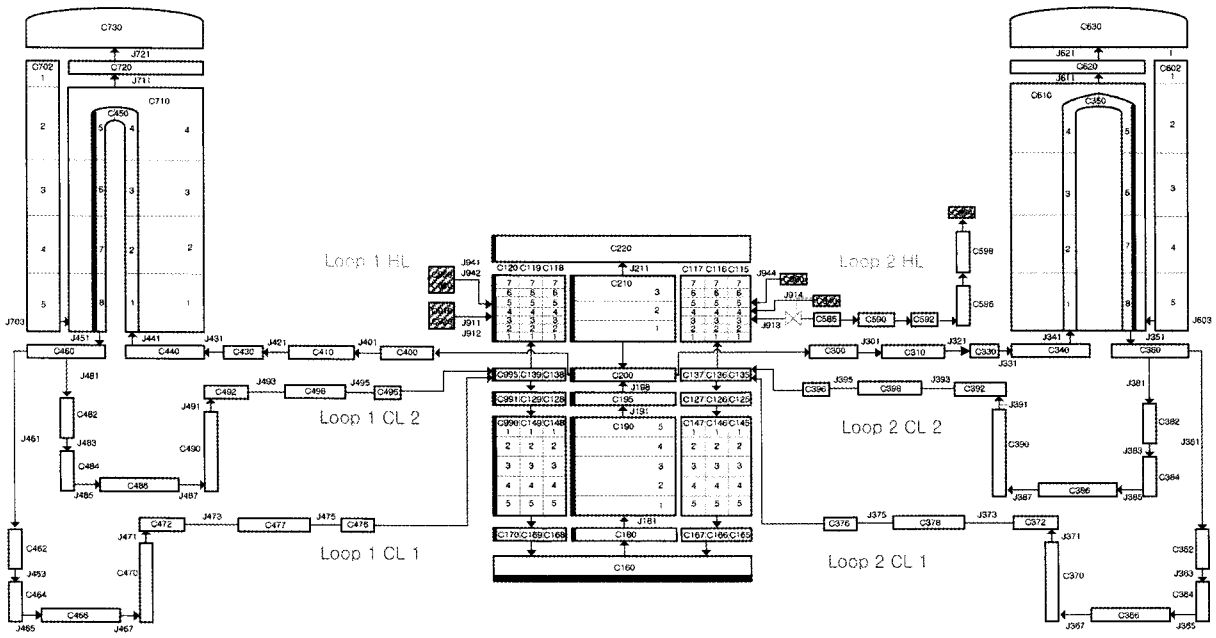

Fig. 23. Schematic Nodalization for the SNUF

(from C115 to C120), and lower downcomer (from C145 to C150).

To simulate the multi-dimensional phenomena in the downcomer, the upper and lower downcomers were divided into six regions in the azimuthal direction. In the vertical direction, the upper and lower downcomers had seven nodes. The cross-junctions connected the neighboring volumes. The RCPs stopped acting as a resistance that increased the differential pressure between the upper plenum and downcomer during the accident in the prototype. To simulate the resistance, the pressure loss coefficients were input to consider a pressure drop through the RCPs (C370, C390, C470, and C490). As a flow boundary, the intact DVI lines (J911, J912, and J914) were connected to the upper downcomer to supply the SI water. The break valve (V913) simulated the DVI line guillotine break. The five pipes (C586, C590, C592, C596, and C598) and the time dependent volume (C954) were utilized to simulate the broken pipeline and the discharge tank. We modeled the core barrel as a heat structure to transfer the heat between the core and downcomer. The test vessel and pipes were modeled as a heat structure to simulate the heat loss to the surroundings. The primary side components of the steam generator included the inlet plenum (C340 and C440), tube region (C350 and C450), and the outlet plenum (C360 and C460). The secondary side consisted of the downcomer (C602 and C702), riser (C610 and C710), separator (C620 and C720), and dome region (C630 and C730).

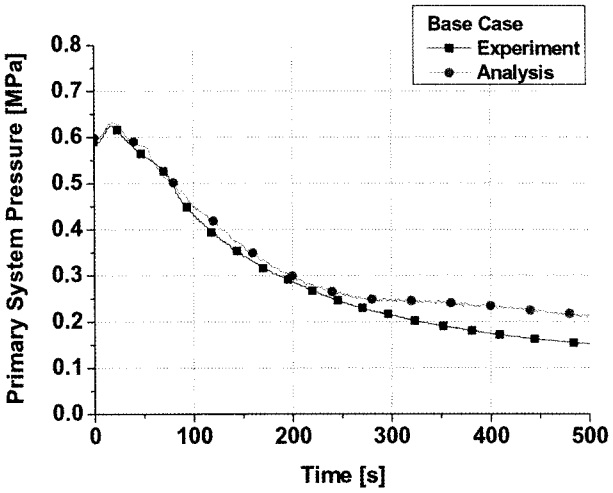

Fig. 24. Primary System Pressure of the Base Case

3.2 MARS Analysis

To validate the capability of the MARS code, three cases among the experiments were simulated with the MARS code, and one of these was the base case for simulating the accident of the prototype. Cases B1 and S2, showing significant deviation compared to the base

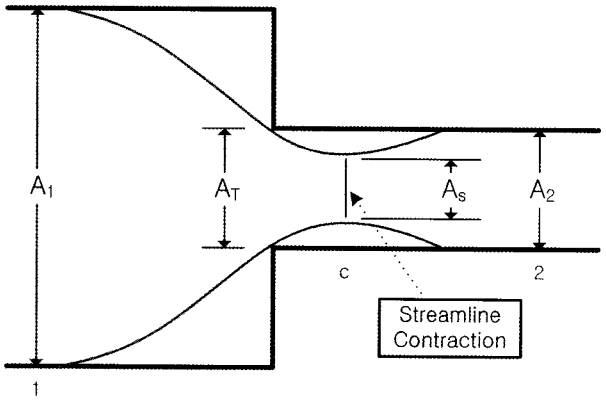

Fig. 25. Schematic Diagram of Streamline Contraction

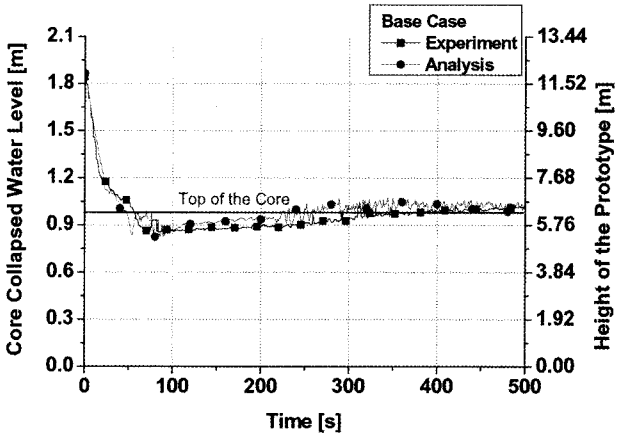

Fig. 27. Core Collapsed Water Level of the Base Case

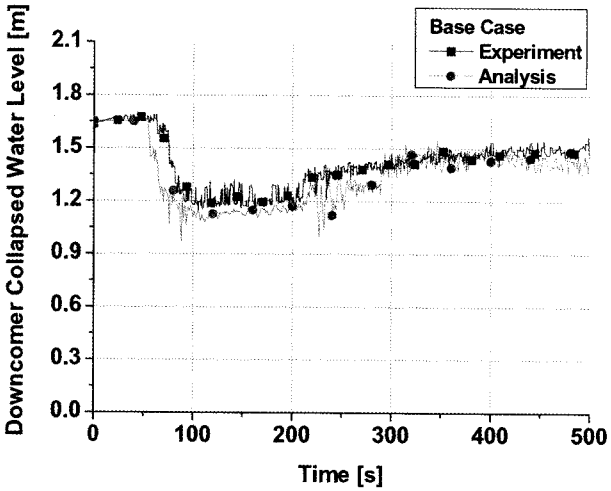

Fig. 26. Downcomer Collapsed Water Level of the Base Case

case, were chosen and analyzed with the MARS code to validate the calculating capability according to the variation of the conditions.

3.2.1 Analysis of the Base Case

The base case was simulated with the MARS code according to the test conditions listed in Table 4. For the analysis, we utilized the nodalization mentioned in Section 3.1. As shown in Fig. 24, the changing rate of the primary system pressure of the experiment was simulated fairly well by MARS code. However, there was a deviation between the experimental result and the analysis result after 250 s. In the SNUF, the broken DVI line was simulated with a pipeline so that the streamline contraction at the break occurred downstream, as shown in Fig. 25. Therefore, the rate of contraction should be considered for realistically simulating the broken DVI line. An equation related to the ratio of contraction was obtained by [16] as follows.

$$\frac{A_s}{A_2} = 0.62 + 0.38\left(\frac{A_2}{A_1}\right)^3 \tag{3}$$

When we considered that the area of the downcomer was significantly larger than the area of the broken DVI line, $(A_2/A_1)^3$ was negligible. A_s/A_2 was determined as being 0.62. To precisely simulate the broken DVI line, we considered the streamline contraction in an incompressible flow. A discharge coefficient of 0.62 was applied according to the contraction ratio. The ratio was inappropriate for predicting the phenomenon when steam was discharged to the broken DVI line because the steam was a compressible flow, unlike the water. After the downcomer seal clearing, a large amount of steam incoming from the cold leg was discharged. As a consequence, the ratio of the streamline contraction may have increased gradually. Thus, a different discharge coefficient, which may be larger than 0.62, should be applied to simulate the break flow during the later period of the accident. However, the same discharged coefficient of 0.62 was applied for the entire period of the accident because the discharge coefficient for simulating the discharge of the steam was not precisely known. Thus, the steam was not sufficiently discharged to the broken DVI line in the MARS analysis. As a result, the primary system pressure of the analysis was maintained at a higher level than that of the test after 250 s. However, the downcomer seal clearing occurred around 70 s so that the deviation of the pressure of the primary system during the later period was not significantly relevant to the major focus of this study.

As shown in Fig. 26, the downcomer collapsed water level was similarly simulated with the MARS code. The decrease of the downcomer collapsed level at 70 s meant that downcomer seal clearing occurred. Thus, we concluded that the downcomer seal clearing was predicted reasonably with the MARS code. The core collapsed water level also was calculated well by MARS code, as shown in Fig. 27. The minimum core collapsed level and the time when it had a minimum level were appropriately predicted by MARS code.

From the above results, we concluded that the base case was generally well simulated with the MARS code. However, from the viewpoint of the discharge coefficient, it was necessary to adopt a model with streamline contraction for simulating the overall phenomena during the accident.

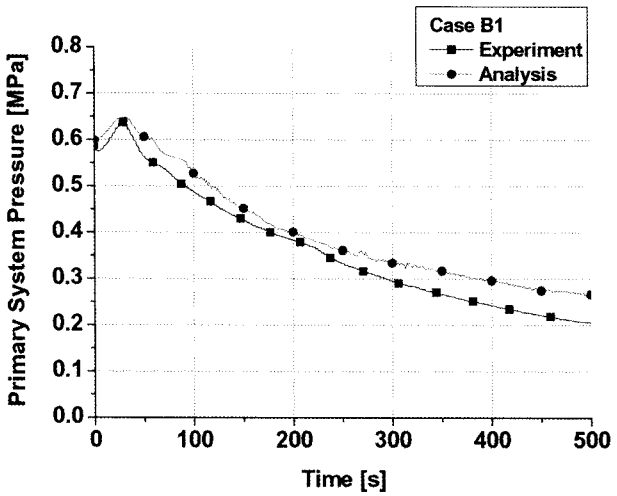

Fig. 28. Primary System Pressure of Case B1

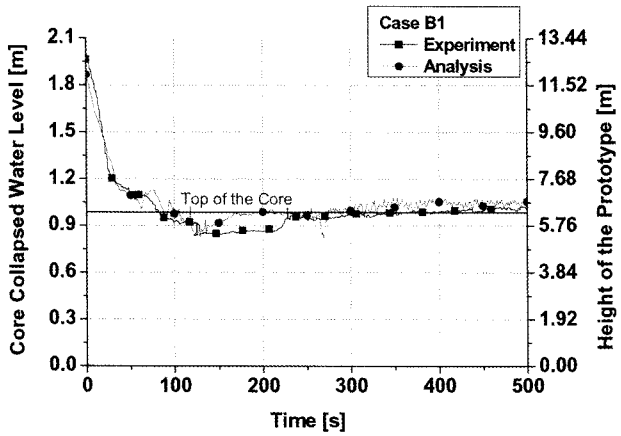

Fig. 29. Core Collapsed Water Level of Case B1

3.2.2 Analysis of the Case of the Reduced Break Area

In the experimental results for case B1 (reduced break area), the primary system pressure was decreased slowly compared to the base case, and the core collapsed water level and the downcomer collapsed water level were observed to be higher than in the base case. Also, the downcomer collapsed water level did not decrease rapidly around 70 s, as it did in the base case, because the downcomer seal clearing obviously did not occur. As compared in Figs. 28-29, the primary system pressure and the core collapsed water level of the MARS analysis results showed similar trends to the experimental results. The deviation of the primary system pressure after 250 s can be explained by the distortion of the discharge coefficient, as described in Section 3.2.1. As illustrated in Fig. 30, the downcomer collapsed water level of the MARS analysis result decreased slowly from 70 s to 150 s without a sharp drop.

However, the result of the downcomer collapsed water level showed some deviation between 100 s and 250 s, as shown in Fig 30. The downcomer collapsed water level, in the analysis result, was maintained at a lower level than in the experimental result. The minimum downcomer collapsed water level was calculated as about 1.2 m, which was the same value as that of the base case. The difference between the MARS analysis and the experiment can be explained by the capability of the MARS code to simulate the bypass flow of the SI water. In the DVI line break accident, the bypass phenomenon meant that some amount of the SI water injected from the DVI line was directly discharged to the broken DVI line by the steam flowing through the upper downcomer.

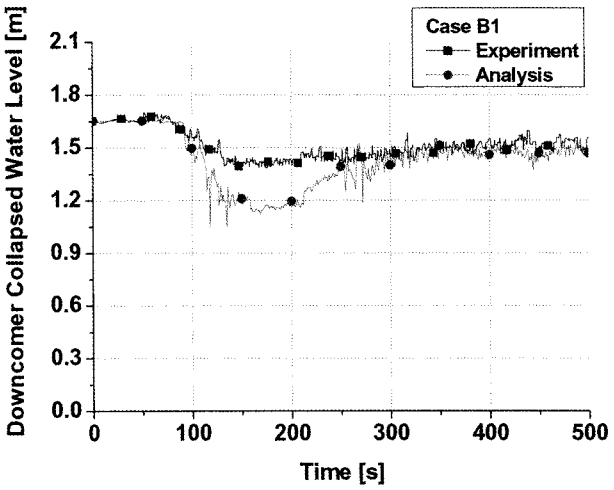

Fig. 30. Downcomer Collapsed Water Level of Case B1

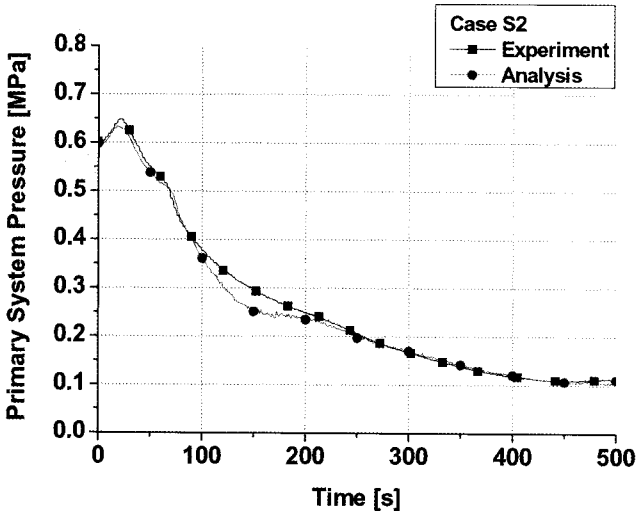

Fig. 31. Primary System Pressure of Case S2

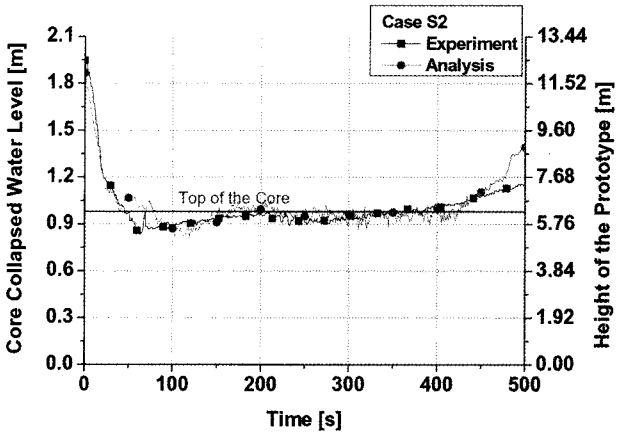

Fig. 33. Core Collapsed Water Level of Case S2

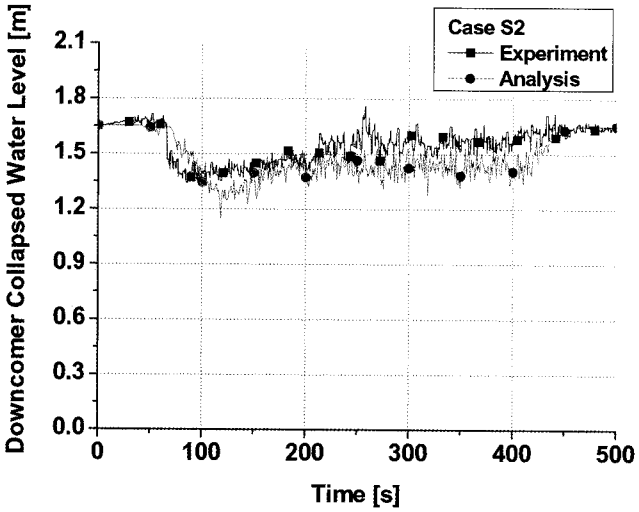

Fig. 32. Downcomer Collapsed Water Level of Case S2

According to a study about the reliable regulatory auditing code [17], when the steam flow rate incoming from the intact cold leg was low, the bypass flow of the SI water was overestimated in the RELAP5 code. The overestimation was induced by the numerical diffusion when utilizing the donor cell upwind scheme and the relatively large node in the RELAP5 code. In case B1, the downcomer seal clearing did not clearly occur due to the small break area so that the steam could not sufficiently pass through the upper downcomer. Thus, the flow rate of the steam in the upper downcomer was low in case B1. Considering that the MARS code was based on adopting the RELAP5 code as a one-dimensional module and the steam flow rate in the experiment of case B1 was low, we expected that the bypass flow rate of the SI water was overestimated in the MARS analysis for case of B1 compared to the actual experiment. Thus, the downcomer collapsed water level was maintained at a low level in the MARS analysis due to the bypass of the SI water. On the other hand, the steam flow from the cold leg may be high in the base case compared to case B1. Therefore, we expected that the bypass flow of the SI water was predicted well in the base case so that the result of the downcomer collapsed water level in the base case agreed reasonably with the experiment.

3.2.3 Analysis of the Case of the Increased SI Flow Rate

In the experiment for case S2 (increased SI flow rate), the primary system pressure decreased rapidly; the downcomer collapsed water level and the core collapsed water level were maintained at a high level compared to the base case. As shown in Figs. 31-33, the result of the MARS analysis showed comparatively similar trends to the experimental results such as the primary system pressure and the core and the downcomer collapsed water level. Therefore, we concluded that the MARS code reasonably predicted the variation of the SI flow rate case.

In the analysis of case S2, the deviation of the pressure by the distortion of the discharge coefficient was not observed because the downcomer collapsed water level was maintained at a relatively high level due to the high SI flow rate. For this reason, the water, not the steam, was mainly discharged to the broken DVI line during the accident period. Therefore, streamline contraction occurred

without changes in the flow characteristics in the sensitivity case so that the discharge coefficient was suitably applied.

4. CONCLUSIONS

In order to understand the thermal hydraulic phenomena in the DVI line break LOCA of the APR1400 reactor, an experimental study was performed with the SNUF. For observing the phenomena according to the various test conditions, we carried out experiments involving eight test cases. The results of the experiments were as follows. The thermal power in the core and the SI flow rate affected significantly the total energy of the primary system so that the primary system pressure and the coolant temperature were governed by two parameters. These parameters also influenced the time of occurrence of the downcomer seal clearing. However, the core collapsed water level was not dependent on the SI flow rate; whereas, it was affected strongly by the thermal power in the core. The discharged flow rate to the broken DVI line, dependent on the break area and the position of the break, played a dominant role in the vent of the steam. Last, the temperature of the SI water did not affect the main phenomena in this study. The experiments for the three test cases were simulated with the MARS code to validate the MARS code. The results of the MARS code analysis showed considerable agreement in terms of being able to simulate the overall thermal hydraulic phenomena, including the downcomer seal clearing. However, the bypass flow of the SI water was overestimated in a region with a low steam flow rate, and the streamline contraction of the two phase flow, not a completely incompressible flow, was not simulated appropriately. Therefore, we require improved models in the MARS code to simulate the DVI line break accident in the APR1400 as well as the SNUF.

ACKNOWLEDGMENTS

This work was supported by KAERI (Korea Atomic Energy Research Institute). The authors would like to thank the staff in the Thermal Hydraulic Safety Research Center of the KAERI for numerous helpful technical discussions.

Nomenclatures

A	Broken DVI area	[m^2]
C	Specific heat	[J/kg/K]
h	Specific enthalpy	[J/kg]
T	Temperature	[K]

Greek Letters

ρ	Density	[kg/m^3]

Subscripts

1	Upstream
2	Downstream
f	Fluid
g	Gas
R	Ratio of the SNUF and prototype model
s	Streamline contraction

REFERENCES

[1] Korea Hydro & Nuclear Power Co., Standard Safety Analysis Report for Advanced Power Reactor 1400, Seoul, Korea, 2002.

[2] J. Liebert, R. Emmerling, "UPTF Experiment – Flow Phenomena during Full-scale Loop Seal Clearing of a PWR," Nuclear Engineering and Design, vol. 179, pp. 51-64, 1998.

[3] Korea Atomic Energy Research Institute, "Best Estimate Small Break Loss of Coolant Analyses for Korean Next Generation Reactor with DVI ECCS," KAERI/TR-1235/99, Daejon, Korea, 1999.

[4] D. J. Euh, H. S. Park, K. Y. Choi, T. S. Kwon, W. P. Baek, "DVI-line break LOCA Analysis of The ATLAS-An Integral Effect Test Loop for Pressurized Water Reactors," Proc. of the 11th International Topical Meeting on Nuclear Reactor Thermal Hydraulics (NURETH-11), Avignon, France, October 2-6, 2005.

[5] B. J. Yun, C. H. Song, K. H. Min, H. K. Cho, G. C. Park, "Experimental Observations of the Hydraulic Phenomena in the APR-1400 Downcomer during the DVI Line Break Accident," Korea Nuclear Society Spring Meeting, 2003.

[6] Y. S. Kim, B. U. Bae, G. C. Park, K. Y. Suh, U. C. Lee, "Experiments and MAAP4 Assessment for Core Mixture Level Depletion after Safety Injection Failure during Long-Term Cooling of a Cold Leg LBLOCA," Nuclear Engineering and Technology, vol.35, no. 2, pp. 91-107, 2003.

[7] Y. S. Kim, B. U. Bae, C. H. Park, G. C. Park, K. Y. Suh, U. C. Lee, "RELAP5/MOD3.3 Analysis of Coolant Depletion Tests after Safety Injection Failure During a Large-Break Loss-of-Coolant Accident," Nuclear Engineering and Design, vol. 235, pp. 2375-2390, 2005.

[8] B. U. Bae, K. H. Lee, Y. S. Kim, B. J. Yun, G. C, Park, "Scaling Methodology for a Reduced-height Reduced-pressure Integral Test Facility to Investigate Direct Vessel Injection Line Break SBLOCA," Nuclear Engineering and Design, vol. 238, pp. 2197-2205, 2008.

[9] J. J. Jeong et al., "Development of a Multi-Dimensional Thermal-Hydraulic System Code, MARS 1.3.1. ," Annals of Nuclear Energy, vol. 26(18), pp.1611-1642, 1999.

[10] Nuclear Regulatory Commission, RELAP5 Code Manual, Bethesda, MD, USA, 1999.

[11] M. J. Thurgood et al., COBRA/TRAC: A Thermal-hydraulics Code for Transient Analysis of Nuclear Reactor Vessels and Primary Coolant Systems, USNRC Report, NUREG/CR-3046, 1983.

[12] American Nuclear Society, Decay Heat Power in Light Water Reactors, ANSI/ANS 5.1-1979, LaGrange Park, IL, USA, 1979.

[13] B. U. Bae, K. H. Lee, Y. S. Kim, B. J. Yun, J. H. Chun, G. C, Park, "An Integral Loop Test and MARS Code Analysis for a DVI Line Break LOCA in the APR1400," Nuclear Engineering and Design, vol. 238, pp. 3336-3347, 2008.

[14] M. M. EL-WAKIL, Nuclear Heat Transport, The American Nuclear Society, La Grange Park, Illinois, USA, 1978
[15] B. J. Yun, H. K. Cho, D. J. Euh, C. H. Song, G. C. Park, "Scaling for the ECC bypass phenomena during the LBLOCA reflood phase," Nuclear Engineering and Design, vol. 231, pp. 315-325, 2004.
[16] Nuclear Regulatory Commission, RELAP5/MOD3.3 Code Manual Volume 1, Washington, DC, USA, 2001.
[17] Korea Institute of Nuclear Safety, Development of Thermal Hydraulic Models for the Reliable Regulatory Auditing Code, KINS/HR-657, Daejon, Korea, 2004.